TOXICOLOGICAL SCIENCES **108(2)**, 273–289 (2009)
doi:10.1093/toxsci/kfp031
Advance Access publication February 20, 2009

Multiple Genes Exhibit Phenobarbital-Induced Constitutive Active/Androstane Receptor–Mediated DNA Methylation Changes during Liver Tumorigenesis and in Liver Tumors

Jennifer M. Phillips* and Jay I. Goodman†,[1]

Department of Biochemistry and Molecular Biology; and †Department of Pharmacology and Toxicology, Michigan State University, East Lansing, Michigan 48824

Received September 26, 2008; accepted February 9, 2009

The constitutive active/androstane receptor (CAR) mediates responses to the nongenotoxic rodent liver tumor promoter phenobarbital (PB), including certain gene expression changes, hepatomegaly, and tumor formation. Aberrant DNA methylation represents epigenetic events that can play multiple roles in tumorigenesis. Previously, 146 unique PB-induced regions of altered DNA methylation (RAMs) were observed in liver tumor–susceptible CAR wild-type (WT) mice (in 23 weeks, precancerous tissue, and 32 weeks, tumor tissue), as compared to the resistant knockout (KO). We believe that at least some of these might be key for tumorigenesis. In the current study, cloning and annotation of a subset (82%) of the unique RAMs revealed 47 genes exhibiting altered methylation; 17 are already implicated in cancer or related processes and, thus, we have identified 30 "new" candidate genes that might be involved in carcinogenesis due to an epigenetic alteration. These may contribute to tumor development through their involvement in angiogenesis, apoptosis, epithelial-mesenchymal cell transition, growth/survival, and invasion/migration/metastasis. We have also, previously, discerned unique PB-elicited RAMs in liver tumor-prone B6C3F1 mice, as compared to the relatively resistant C57BL/6 strain, at 2 or 4 weeks, and identified 51 genes exhibiting altered methylation. Importantly, 11 of these genes were identified from identical, unique RAMs discerned in both the sensitive B6C3F1 and CAR WT mice, thus representing an initial, potential candidate "fingerprint" which might serve as a biomarker for PB-induced tumorigenesis. These two studies reveal "new" genes whose epigenetic statuses changed uniquely in liver tumor–susceptible mice (B6C3F1 and CAR WT), as compared to their resistant counterparts (C57BL/6 and CAR KO, respectively), within a continuum of PB-induced tumorigenesis.

Key Words: **CAR; constitutive active/androstane receptor; DNA methylation; epigenetic; mouse liver tumors; phenobarbital.**

The constitutive active/androstane nuclear receptor (CAR) is expressed primarily in the liver and mediates transcription of drug-metabolizing enzymes, for example, cytochrome P450 (CYP) 2B10 and CYP3A11, plus NADPH-cytochrome reductase (Ueda *et al.*, 2002), the UDP-glucuronosyltransferase UGT1A1 (Sugatani *et al.*, 2001), and glutathione *S*-transferases (Huang *et al.*, 2003). Thus, CAR plays a key role in the metabolism and excretion of xenobiotics and endobiotics (e.g., bilirubin and bile acids), in addition to xenobiotic-induced changes in energy metabolism (reviewed in Konno *et al.*, 2008).

Phenobarbital (PB), the prototypical nongenotoxic rodent liver tumor promoter, causes liver hyperplasia and hypertrophy, and induces xenobiotic-metabolizing enzymes (Whysner *et al.*, 1996). A promoting dose of PB increases DNA synthesis and decreases apoptosis in murine hepatocytes (Kolaja *et al.*, 1996b), and initially stimulates hepatocyte proliferation (Counts *et al.*, 1996; Kolaja *et al.*, 1996a). Ha-*ras* mutations are infrequent in PB-induced mouse liver tumors (Fox *et al.*, 1990; Rumsby *et al.*, 1991), however, hypomethylation of Ha-*ras* (Vorce and Goodman, 1991), and increased expression occurs (Counts *et al.*, 1997). Additionally, connexin 32 (the major gap junction-forming protein in liver) is required for promotion by PB (Moennikes *et al.*, 2000).

PB and PB-like compounds (e.g., 1,4-bis[2-(3,5-dichloropyridyloxy)]benzene, TCPOBOP) activate CAR (reviewed in Swales and Negishi, 2004). CAR is required for PB-induced hepatomegaly and *Cyp2b10* gene expression in mouse liver (Wei *et al.*, 2000), and chronic CAR activation in response to PB or TCPOBOP results in hepatocarcinogenesis (Huang *et al.*, 2005). Importantly, CAR is essential for tumor promotion by PB in diethylnitrosamine (DEN)–initiated C3H/He mice (Yamamoto *et al.*, 2004). Microarray data analysis of PB-treated CAR wild-type (WT) and knockout (KO) mice indicated that of 138 genes (out of 8736 total genes/expressed sequence tags whose expression was altered, only approximately half of these changes were CAR dependent (Ueda *et al.*, 2002). In response to PB treatment, CAR translocates from the cytoplasm to the nucleus, heterodimerizes with retinoid X receptor, and binds to and activates transcriptional elements (e.g., PB-responsive enhancer modules) to affect gene expression (Honkakoski *et al.*, 1998;

[1] To whom correspondence should be addressed at Department of Pharmacology and Toxicology, Michigan State University, B-440 Life Sciences Bldg., East Lansing, MI 48824. Fax: (517) 353-8915. E-mail: goodman3@msu.edu.

Kawamoto *et al*., 1999; Sueyoshi *et al*., 1999). Nuclear translocation of CAR can be blocked by an inhibitor of protein phosphatase 2A (PP2A) (Kawamoto *et al*., 1999), whereas a subunit of protein phosphatase 1, PPP1R16A, can inhibit protein phosphatase 1-beta (PP1β), resulting in CAR translocation (Sueyoshi *et al*., 2008). Additionally, CAR-mediated induction of the *Cyp2b10* gene can be blocked by a Ca^{2+}/calmodulin-dependent kinase inhibitor, without affecting nuclear accumulation (Yamamoto *et al*., 2003). These results suggest that both phosphorylation and dephosphorylation events contribute to CAR activation. We speculate that enhancement of PP2A and/or inhibition of PP1β plays a role in the mechanism by which PB stimulates nuclear translocation of CAR.

DNA methylation is an epigenetic mechanism regulating transcription which, when altered, may lead to tumorigenesis. For instance, hypomethylation can activate oncogenes, whereas hypermethylation can silence tumor suppressors (Esteller, 2008; Goodman and Watson, 2002). Therefore, aberrant methylation, in addition to mutation, can play critical roles during all stages of tumor formation, for example, by facilitating the progressive clonal expansion of subpopulations which possess growth advantages over neighboring cells (Goodman and Watson, 2002). Although the detailed mechanisms of PB-induced altered DNA methylation remain to be elucidated, liver tumor-sensitive B6C3F1 mice, as compared with resistant C57BL/6, appear to be "defective" with regard to the ability to preserve normal methylation patterns (Watson and Goodman, 2002). Indeed, PB causes the formation of unique regions of altered DNA methylation (RAMs) in B6C3F1, compared with C57BL/6, mice at 2 and 4 weeks of treatment (Bachman *et al*., 2006b). Cloning and annotation of these unique RAMs revealed changes in methylation which occurred within genes that are known to play important roles in tumorigenesis (e.g., angiogenesis, invasion, metastasis, and epithelial-mesenchymal cell transition), plus genes which had not previously been linked to cancer, thus providing insight regarding specific genes which may play a role in PB-induced tumorigenesis due to altered DNA methylation (Phillips and Goodman, 2008).

In an analogous fashion to Bachman *et al*. (2006b), Phillips *et al*. (2007) compared DNA methylation patterns in liver tumor–susceptible C3H/He CAR WT mice and resistant CAR KO mice. Unique RAMs in the livers of CAR WT mice initiated with DEN and treated with PB for 23 (precancerous tissue) or 32 (tumor tissue) weeks, compared with CAR KO mice initiated with DEN and treated with PB for 23 weeks, were identified. Methylation changes also occurred in the CAR KO, PB-treated mice, suggesting, analogous to gene expression changes observed in Ueda *et al*. (2002), that DNA methylation changes are both CAR dependent and independent. We hypothesize that a subset of the unique RAMs in the precancerous and tumor tissue are important for facilitating tumorigenesis. In this study, unique RAMs detected in the precancerous and tumor tissue (Phillips *et al*., 2007) were cloned and annotated to discern the particular genes involved and how they might contribute to tumorigenesis, for example, common cellular targets of the genes of interest were identified in order to picture how they might interact to affect critical signaling pathways, leading to key alterations in phenotype. Although Phillips and Goodman (2008) focused upon genes involved in PB-induced tumor formation at very early treatment times (i.e., 2 and 4 weeks), the current study elucidated genes involved at later times, when foci (23 weeks, PB-treated CAR WT) and tumors (32 weeks, PB-treated CAR WT) are apparent. Taken together, these two studies (the aforementioned B6C3F1-C57BL/6 study, and the current CAR study) lead to the identification of genes whose methylation statuses changed uniquely in liver tumor–susceptible mice (B6C3F1 and CAR WT), as compared with their resistant counterparts (C57BL/6 and CAR KO, respectively), within a continuum of PB-induced tumorigenesis.

MATERIALS AND METHODS

Animals, Treatments, and Tissue Samples

The DNA employed for these studies was isolated from the same liver samples used by Phillips *et al*. (2007), and these samples were provided by Yamamoto *et al*. (2004). CAR WT or CAR KO mice, on a C3H/He background (which is highly susceptible to liver tumorigenesis (Buchmann *et al*., 1991), were injected with a single intraperitoneal dose of DEN, 90 mg/kg, at 5 weeks of age and then administered drinking water (control) or 0.05% PB (wt/wt) in drinking water starting at 7 weeks of age and continuing for 23 or 32 weeks, resulting in the following groups: CAR KO, 23-week control, CAR KO, 23-week PB, CAR WT, 23-week control, CAR WT, 23-week PB (precancerous tissue), and CAR WT, 32-week PB (tumor tissue) (Yamamoto *et al*., 2004).

Protocol Employed for the Annotation of PB-Induced Unique Rams in Precancerous and Tumor Tissue

The RAMs cloned and annotated in the current study were previously detected via an approach involving methylation-sensitive restriction digestion, arbitrarily primed PCR (AP-PCR), and capillary electrophoresis (CE) (Supplemental Fig. S1, originally from Phillips *et al*., 2007), a technique described in detail by Bachman *et al*. (2006a). The following comparisons were previously made between experimental groups: (1) the CAR KO, 23-week PB data were compared with the CAR KO, 23-week control data, and (2) both the CAR WT, 23-week PB (precancerous tissue) and CAR WT, 32-week PB (tumor tissue) data were compared with the CAR WT, 23-week control data. For each specific PCR product size that was observed in control versus PB-treated an individual Student's *t*-test was performed to evaluate whether or not there was a statistical ($p < 0.05$) difference in the peak area. Additionally, new methylations (PCR products which were observed in the PB-treated and not in control), as well as 100% hypomethylations (PCR products which were observed in control but not seen at all in PB treated), were viewed as being "significant" (Bachman *et al*., 2006a).

For the methylation analysis performed by Phillips *et al*. (2007), whole liver from four of the five (not including the WT, 32-week PB) groups was utilized; the precancerous liver tissue (WT, 23-week PB) contained no tumors, however, based upon histology of adjacent tissue, there are expected to be very numerous microscopic foci of cellular alteration diffused throughout the tissue. Importantly, DNA was isolated from individual liver tumors that developed in the WT, 32-week PB group.

The 23-week PB-treated mice are 30 weeks of age (PB treatment started when the animals were 7 weeks old), and the 32-week mice are 39 weeks of age. Thus, the mice were past the juvenile development stage and not into old age, and at an age where a reasonable degree of stability of methylation might be anticipated over a 9-week period.

Cloning and sequencing of AP-PCR products. AP-PCR products were first cloned using an in-gel approach to identify in what regions of the genome the PB-induced unique precancerous and tumor RAMs occurred. The AP-PCR products and a 100 base pair DNA ladder (Invitrogen, Carlsbad, CA) were electrophoresed through a 3% NuSieve GTG low melting temperature agarose gel (Lonza Biosciences, Basel, Switzerland). Portions of the gel that contained PCR products within 100 base pair size ranges were excised, melted and used for in-gel cloning reactions prepared with the pGEM-T Easy Vector Kit (Promega, Madison, WI). Clones that contained PCR product inserts were purified and sequenced at the Research Technology and Support Facility at Michigan State University. Sequencing reactions were prepared using either SP6 or T7 sequencing primers (as described in the pGEM-T Easy Vector Technical Manual; Promega, Madison, WI) and subsequently run on an ABI 3730×*l*Genetic Analyzer.

Comparison of the sizes of cloned and sequenced AP-PCR products to the sizes of unique RAMs. After the sequences were obtained, the sizes of the cloned products were compared with the sizes of the unique RAMs in order to determine which cloned products represented unique precancerous and tumor RAMs. In many instances, it can be confidently stated that a particular cloned product represents a single RAM and as such, the methylation status of that RAM is unambiguous. However, the raw data analysis performed to establish if a RAM occurred in a treatment group as compared with its respective control group (Phillips *et al*., 2007) is based upon the understanding that the ABI 3130 Genetic Analyzer capillary electrophoresis instrument does not detect PCR product sizes with 100% accuracy. Therefore, in certain instances during the analysis of the raw data, PCR product sizes were combined. Six animals per experimental group were used and restriction digestions were performed in duplicate, followed by AP-PCR, for a total of 12 reactions. If multiple PCR product sizes within two base pairs of one another displayed product in less than half of the 12 AP-PCR reactions, these products were considered to be "identical" and were subsequently combined. This procedure has implications for analysis of the cloning data. For example, two RAMs occurred uniquely in the tumor tissue as a result of *Rsa*I/*Hpa*II digestion: a hypomethylation at 402 bp and a carry forward new methylation at 404 bp (Supplemental Fig. S1). A carry forward methylation change is a unique RAM that was observed in both precancerous and tumor tissue. A PCR product of 404 bp was cloned, and a BLAT search showed that the product spans an intronic region within the transmembrane protein 132d (*Tmem132d*) gene (Table 1). Due to our basic data analysis ± 2 bp assumption, the methylation status of *Tmem132d* is ambiguous; it could represent the hypomethylated RAM at 402 bp or the newly methylated carry forward RAM at 404 bp.

Additionally, the use of three different methylation-sensitive enzyme pairs could also reveal multiple methylation statuses of a particular gene. In the case of dipeptidylpeptidase 10 (*Dpp10*), *Rsa*I/*Hpa*II digestion revealed a hypomethylated RAM, whereas *Rsa*I/*Msp*I digestion demonstrated a carry forward hypermethylated RAM in the precancerous tissue (Table 1). Thus, *Dpp10* could represent one or both of these RAMs because different restriction digestions were utilized, each of which reveals information regarding the methylation patterns of different cytosines at and within the sites of primer annealing. The "methylation status" data column in Table 1 reflects these 2 situations (e.g., Hypo/New for a single gene, in a particular tissue).

Analysis of sequenced AP-PCR products. The sequences were subjected to BLAT database searches of the mouse genome (UCSC Genome Browser, July 2007 mouse assembly (http://genome.ucsc.edu/cgi-bin/hgBlat?command=start&org=mouse) in order to ascertain in which regions of the genome the unique PB-induced precancerous and tumor RAMs occurred. The BLAT program aligns a nucleotide or amino acid sequence to an index of an entire animal genome. For DNA sequence queries, BLAT can detect sequence alignments of 95% or greater similarity of regions with lengths of 25 or more base pairs. Additional information about the genomic region/gene is listed, including, but not limited to: gene information, sequence conservation between species, GC percentage, and the location of single nucleotide polymorphisms and repeat elements. The unique RAMs were classified according to a scheme that indicates where, in relation to a gene (e.g., within an intron, within an exon, upstream of the transcriptional start site), they are located. RAMs were also categorized by chromosomal location and gene function. Gene Ontology information for Supplemental Figure S5 was obtained from http://www.geneontology.org/.

The functions of the genes identified using BLAT searches were investigated via Pathway Studio 5.0 (Ariadne Genomics, Rockville, MD). In this fashion, connections between each individual gene and other genes, cellular processes, or disease states were elucidated. For a subset of the genes, examples of these analyses are located in Supplemental Figures S6-S9. In addition, common targets and common regulators of genes identified from unique RAMs in both the precancerous and tumor tissue were discerned. Pathway Studio 5.0 was also utilized to uncover documented links between unique precancerous and tumor RAMs and cancer-related processes, including angiogenesis, apoptosis, epithelial-mesenchymal cell transition (EMT), migration/invasion/metastasis and growth and survival.

Comparison of Genes/Genomic Regions Identified from Unique PB-Induced RAMs that Formed in both CAR WT (Precancerous Liver and/or Liver Tumor) to Genes/Genomic Regions Identified from Unique PB-induced RAMs in Liver Tumor–Susceptible B6C3F1 Mice (2 and/or 4 Weeks)

We previously identified 170 total unique RAMs in livers of tumor-susceptible B6C3F1 mice treated with 0.05% (wt/wt) PB for 2 or 4 weeks, as compared with the resistant C57BL/6 stock (Bachman *et al*., 2006b), and PCR products representing 90 of these 170 (53%) RAMs were cloned and subjected to BLAT searches that resulted in 51 annotated genes (Phillips and Goodman, 2008). Unique B6C3F1 RAMs at 2 and 4 weeks, which corresponded to identical genes and uncharacterized regions (i.e., regions of DNA greater than 10 kb away from an annotated gene) observed in the current study, were compared with the unique CAR precancerous and tumor RAMs, in order to determine whether the methylation patterns of common genes/uncharacterized regions observed in both studies were altered similarly or differently by PB treatment. Because three different restriction digestions were utilized, multiple RAMs might represent the same gene/uncharacterized region.

The following criteria needed to be met in order for a gene/uncharacterized genomic region identified from a PB-induced RAM to be viewed as being in common between the studies: (1) the RAM must have been cloned in both the B6C3F1 (2 and/or 4 weeks PB) and CAR WT (precancerous and/or tumor) mice, and (2) the unique RAMs in the B6C3F1 and CAR WT mice must have aligned to the same region of the genome. Hypermethylated RAMs (significant increases, Student's *t*-test, $p < 0.05$) and newly methylated RAMs are considered to be increases in methylation, whereas hypomethylated RAMs (both 100% decreases, and those which are significant, Student's *t*-test, $p < 0.05$) are considered to be decreases. Genes and uncharacterized genomic regions, identified from identical, unique PB-induced RAMs that formed in both CAR WT (precancerous liver and/or liver tumor) and B6C3F1 (2 and/or 4 weeks treated), are listed in Table 3 and Supplemental Table S3, respectively.

Cloning and sequencing revealed two observations regarding criterion number 2 (above). First, following digestion with the same methylation-sensitive restriction enzyme, PCR products occasionally formed which (1) represented distinct RAMs that differed by more than 2 bp in multiple groups (B6C3F1, 2 and/or 4 weeks, and CAR WT, precancerous liver and/or liver tumor) and (2) aligned to the same region of the genome. Second, following digestion with the same methylation-sensitive restriction enzyme, PCR products occasionally formed which (1) represented distinct RAMs that were within 2 bp of one another (e.g., unique RAMs at 315 and 317 bp) in multiple groups (B6C3F1, 2 and/or 4 weeks, and CAR WT, precancerous liver and/or liver tumor) and (2) aligned to the same region of the genome. Thus, for a particular restriction digestion, unique RAMs in the B6C3F1 and CAR WT

TABLE 1

Genes and Genomic Regions Identified from Unique PB-induced RAMs in C3H/He CAR WT (Precancerous Liver and/or Liver Tumor), as compared with Resistant PB-Treated KO Mice, were Cloned and Subjected to BLAST-like Alignment Tool (BLAT) Searches

Methylation status[a]							
Precan.[b]	Tumor[c]	Gene name	Gene symbol	Accession number	Genomic location[d]	Normal function	Potential role in tumorigenesis
	Hypo (M)[e]	Cellular retinoic acid binding protein 1	*Crabp1*	NM_013496	1.A.ii	Retinoic acid (RA) metabolism (1)[f]	Methylation-associated silencing in esophageal carcinoma (2)
	Hypo (M)	NudC domain containing 3	*Nudcd3*	NM_173748	1.A.ii	Dynein stabilization and cell viability (3)	—
	Hypo (M)	Protein kinase C, epsilon	*Prkce*	NM_011104	1.A.iii	Inhibition of apoptosis (4) and cell proliferation (5)	Transformation (6) and cancer cell proliferation (7)
	Hypo (M)	p53 and DNA damage regulated 1	*Pdrg1*	NM_178939	1.C.ii	Facilitates ultraviolet radiation-induced cell death (8)	—
	Hypo (M)	Solute carrier family 11 (proton-coupled divalent metal ion transporters), member 2	*Slc11a2*	NM_008732	1.A.iii	Divalent cation transport (9)	Overexpressed during the progression of esophageal adenocarcinoma (10)
	Hypo (M)	Spermatogenesis associated 21	*Spata21*	NM_177867	1.B.i	Unknown	—
	Hypo (M)	Tubulin tyrosine ligase-like family, member 9 (381 bp)	*Ttll9*	NM_029064	1.A.ii	α-Tubulin-preferring glutamyl ligase (11)	—
	Hypo (B)	Solute carrier family 38, member 9	*Slc38a9*	NM_178746	1.A.iii	Unknown	—
Hypo (B)[g]	**Hypo (B)**	Annexin A4	*Anxa4*	NM_013471	1.A.i	Ca^{2+}-regulated protein involved in ion conductance (12) and membrane permeability (13)	Promotes migration in a model system of renal carcinoma (14)
Hypo (B)	**Hypo (B)**	Coiled-coil domain containing 134	*Ccdc134*	NM_172428	1.A.i	Secretory protein that inhibits ERK and JNK activation (15)	Expressed in a variety of human tumor tissues (15)
Hypo (B)	**Hypo (B)**	Exosome component 2	*Exosc2*	NM_144886	1.C.i	Putative exosome component (16)	—
Hypo (M)	**Hypo (M)**	RIKEN cDNA 1700027D21 gene	*1700027D21Rik*	NM_029661	1.C.i	Unknown	—
Hypo (B)	**Hypo (B)**	c-abl oncogene 1, receptor tyrosine kinase	*Abl1*	NM_009594	1.B.ii	Cell cycle arrest (17), apoptosis (18), and DNA synthesis in response to growth factors (19)	Various oncogenes are derived from c-abl (20)
Hypo (H)	**Hypo (H)** or Hypo (H)[h]	DNA segment, Chr 13, Wayne State University 177, expressed	*D13Wsu177e*	NM_178605	1.B.i	Unknown	—
Hypo (H)	**Hypo (H)** or Hypo (H)[h]	HIG1 domain family, member 2A	*Higd2a*	NM_025933	1.A.i	Unknown	—
Hyper (M)	Hypo (B)	Dead box polypeptide 54	*Ddx54*	NM_028041	1.A.iii	Corepressor of nuclear receptors (21)	—
Hyper (H)	Hyper (M)	Yip1 interacting factor homolog A (S. cerevisiae)	*Yif1a*	NM_026553	1.A.ii	In yeast, functions in endoplasmic reticulum-to-Golgi transport (22)	—
New (M)		Branched chain aminotransferase 2, mitochondrial	*Bcat2*	NM_009737	1.A.ii	Metabolism of branched chain amino acid (23)	—
New (M)		Ubiquinol-cytochrome c reductase (6.4 kD) subunit	*Uqcr*	NM_025650	1.A.i	Unknown	—
New (M)		Zinc finger and BTB domain containing 8 opposite strand	*Zbtb8os*	NM_025970	1.A.iii	Unknown	—

TABLE 1—*Continued*

Methylation status[a]							
Precan.[b]	Tumor[c]	Gene name	Gene symbol	Accession number	Genomic location[d]	Normal function	Potential role in tumorigenesis
New (B)	New (B)	Chimerin (chimaerin) 2	*Chn2*	NM_023543	1.A.iii	Regulation of smooth muscle cell proliferation/migration (24) and T-cell responses (25)	Inhibition of proliferation in breast cancer cells (26)
New (B)	New (B)	RIKEN cDNA 1520401A03 gene	*1520401A03Rik*	NM_177132	1.A.iii	Unknown	—
New (M)	New (M)	Sine oculis-related homeobox 3 homolog (Drosophila)	*Six3*	NM_011381	1.A.ii	Homeobox gene involved in brain (27) and ocular (28) development	—
	New (B)	A disintegrin-like and metallopeptidase (reprolysin type) with thrombospondin type 1 motif, 17	*Adamts17*	NM_001033877	1.A.iii	Unknown	—
	New (H)	Annexin A2	*Anxa2*	NM_007585	1.A.iii	Osteoblastic mineralization (29), signal transduction (30) and proliferation (31)	Expression in prostate cancer cells inhibits migration (32)
	New (H)	BTB (POZ) domain containing 11	*Btbd11*	NM_028709	1.A.iii	Potential role in nervous system development (33)	—
	New (H)	Chemokine (C-C- motif) receptor 4	*Ccr4*	NM_009916	1.A.iii	Normal immunity (34)	Tumor immunity (34)
	New (B,H)[i]	Calsyntenin 2	*Clstn2*	NM_022319	1.A.iii	Potential role in synaptic transmission (35)	—
	New (B,H)[i]	Folliculin	*Flcn*	NM_146018	1.A.iii	Potential role in energy and/or nutrient sensing (36)	Potential tumor suppressor (37)
	New (M)	Glutamate decarboxylase-like 1	*Gadl1*	XM_135211	1.A.iii	Unknown	—
	New (B)	Hect domain and RLD 3	*Herc3*	NM_028705	1.A.ii	Binds to and is regulated by ubiquitin (38)	—
	New (B)	Like-glycosyltransferase	*Large*	NM_010687	1.A.iii	Posttranslational protein modification (39), brain development (40)	Located within a critical region that is deleted in meningiomas (41)
	New (B)	Leucine rich repeat and Ig domain containing 2	*Lingo2*	NM_175516	1.A.iii	Unknown	—
	New (H,M)[i]	Src-related kinase lacking C- and N-terminal myristylation sites	*Srms*	NM_011481	1.A.i	Nonreceptor tyrosine kinase (42)	—
	New (B,H)[i]	Transcription factor 4	*Tcf4*	NM_013685	1.A.iii	Wnt signaling (43)	Expression increased in cancer (44,45)
	New (B)	Tubulin tyrosine ligase-like family, member 9 (208 bp)	*Ttll9*	NM_029064	1.A.ii	α-Tubulin–preferring glutamyl ligase (11)	—
	New (M)	WD repeat domain 17	*Wdr17*	NM_028220	1.A.iii	Potential role in eye development (46)	—
	New (H)	Zinc finger and SCAN domain containing 22	*Zscan22*	NM_001001447	1.A.i	Unknown	—
	New (H)	RIKEN cDNA A430078G23 gene	*A430078G23Rik*	NM_001033378	1.B.i	Unknown	—
	Hypo (B,H,M) and/or New (H)[h,i]	Protein tyrosine phosphatase, receptor type O	*Ptpro*	NM_011216	1.A.iii	Transmembrane protein tyrosine phosphatase (47)	Tumor suppressor (47)

TABLE 1—*Continued*

Methylation status[a]							
Precan.[b]	Tumor[c]	Gene name	Gene symbol	Accession number	Genomic location[d]	Normal function	Potential role in tumorigenesis
New (M)	Hypo (M)	WSC domain containing 1 (407 bp)	*Wscd1*	NM_177618	1.A.iii	Unknown	—
Hypo (H) and/or **Hyper (M)**[i]	**Hyper (M)**	Dipeptidylpeptidase 10	*Dpp10*	NM_199021	1.A.iii	Regulation of K^+-gated voltage channels (48)	—
Hypo (H) and/or **Hyper (M)**[i]	**Hyper (M)**	Tyrosine kinase nonreceptor 2	*Tnk2*	NM_016788	1.A.iii	Intracellular kinase that might be involved in growth/movement (49)	Invasion and metastasis (50)
Hypo (B) and/or Hyper (M)[i]	**Hypo (B)** and/or Hypo (M)[i]	Ephrin B2	*Efnb2*	NM_010111	1.A.iii	Vascular development, angiogenesis in adult mice (51)	Angiogenesis and invasion(51–53)
New (H)	**New (H)** or Hypo (H)[h]	Predicted gene, EG622408	*EG622408*	NM_001037914	1.C.i	Unknown	—
Hypo (H) or Hyper (H)[h]	Hypo (B,H) and/or New (M)[i]	Prickle-like 2 (Drosophila)	*Prickle2*	NM_001081146	1.B.ii	Tissue/planar polarity via the WNT/PCP signaling pathway (54)	Expression detected in gastric and uterine cancers (55)
Hypo (B) and/or Hyper (M)[i]	**Hypo (B)** and/or Hypo (M)[i]	Triple functional domain (PTPRF interacting)	*Trio*	XM_001474968	1.A.ii	Coordination of cytoskeleton remodeling (56)	Growth, invasion, tumorigenicity (57)
New (M) and/or **New (H)**[i]	Hypo (M,H) and/or **New (H)**[h,i]	Transmembrane protein 132d	*Tmem132d*	NM_172885	1.A.iii	Unknown	—
Hyper (H) and/or New (B)[i]	Hypo (B,H,M) and/or New (H)[h,i]	WSC domain containing 1 (359–361 bp)	*Wscd1*	NM_177618	1.A.iii	Unknown	—
Hypo in precan. or tumor (B/H/M)		Uncharacterized[j]	5 RAMs	—	2	—	—
Hyper in precan. or tumor (B/H/M)		Uncharacterized[j]	3 RAMs	—	2	—	—
New in precan. or tumor (B/H/M)		Uncharacterized[j]	9 RAMs	—	2	—	—
Methylation statuses are opposite in precan versus tumor		Uncharacterized[j]	1 RAM	—	2	—	—
Precan. status is ambiguous[h,i]		Uncharacterized[j]	2 RAMs	—	2	—	—
	Tumor status is ambiguous[h,i]	Uncharacterized[j]	3 RAMs	—	2	—	—
Hypo (B)	Hypo (M)	Multiple gene hits[k]	442–445 bp	Various	3	Various	Various
New (M)		Multiple gene hits[k]	462 bp	Various	3	Various	Various
	New (M)	Uncharacterized[j]	491 bp	—	4	—	—

[a]The methylation status of a region of the genome as determined by Phillips *et al.* (2007), in the treatment group as compared with the control group: hypomethylations are decreases which were statistically significant (Student's *t*-test, $p < 0.05$) plus complete 100% decreases, hypermethylations are increases which were statistically significant (Student's *t*-test, $p < 0.05$), and new methylations were increases, in which specific PCR products formed in the treatment but not in the control group.

[b]Methylation statuses of regions of the genome in precancerous tissue (23 weeks of PB treatment).

[c]Methylation statuses of regions of the genome in tumor tissue (32 weeks of PB treatment).

[d]Genomic location relative to the transcriptional start site.

[e]The letter in parentheses indicates which methylation-sensitive restriction enzyme (*Bss*HII, *Hpa*II, or *Msp*I) led to the identification of the RAM.

[f]The numbers in parentheses correspond to references which are listed in Supplemental Table S1.

[g]Carry forward RAM (listed in bold) was observed in both the precancerous and tumor tissue.

[h]Indicates that the region of the genome might be represented by one of 2 RAMs, that formed via the same restriction digestion and the reason for this uncertainty is explained in the methods.

[i]The region of the genome might be represented by more than one RAM because different restriction digestions (e.g. *Hpa*II, and/or *Msp*I and/or *Bss*HII) led to the identification of multiple RAMs represented by PCR products that aligned to the same region of the genome. With the exception of *Efnb2* and *Trio*, ''and/OR'' indicates that at least 2 of these RAMs exhibited changes in the oppoite direction.

[j]The uncharacterized genomic regions that these RAMs represent are greater than 10 kb away from an annotated gene.

[k]BLAT showed multiple top hits for the particular PCR product and the sequence associates with a specific repeat element.

mice that were within 2 bp of one another or more than 2 bp apart, which were represented by PCR products that aligned to the same region of the genome, were considered to be one RAM. This is evident in Table 3 and Supplemental Table S3. The following is an example of situation number 1, above. A PCR product, representing a 464-bp RAM that was identified after *RsaI*/*MspI* digestion and AP-PCR, was cloned in the B6C3F1 mice at 4 weeks, and

aligned to *Bcat2* (Table 3). Similarly, in the CAR precancerous tissue, a PCR product, representing a 468-bp RAM that was identified after *RsaI/MspI* digestion and AP-PCR, was cloned in the CAR precancerous tissue, and aligned to the same region of *Bcat2* (Table 3). Although the two RAMs were not within 2 bp of one another, the sequencing results clearly demonstrated that the PCR products aligned to the same region of the genome. Therefore, these RAMs were considered to be one RAM. The following is an example of situation number 2, above. For *Ddx54* (Table 3), two distinct RAMs (M315 in precancerous tissue, and M317 in the B6C3F1 mice at 4 weeks) that the cloned PCR products represent were within 2 bp of one another. Therefore, these RAMs were considered to be one RAM.

RESULTS

PCR products were cloned that represent 119 (82%) of the 146 total unique RAMs previously detected in the livers of male C3H/He CAR WT mice treated with a tumor-promoting dose of PB for 23 (precancerous tissue) or 32 (tumor tissue) weeks, as compared with resistant CAR KO mice, including 14 carry forward RAMs (i.e., those which were observed in both the precancerous and tumor tissue) (Supplemental Fig. S1) (Phillips *et al*., 2007). These RAMs were annotated via the BLAT sequence alignment tool, and 47 genes were discerned (Table 1). Two genes (*Ttll9* and *Wscd1*) are listed twice because in each situation, two PCR products of different sizes aligned to two distinct, separate regions of the same gene. Literature references in Table 1 are listed in Supplemental Table S1. RAMs were also classified based on their location relative to an annotated gene (Table 1 and Supplemental Figs. S2 and S3) and chromosomal distribution (Supplemental Fig. S4). All of the annotated genes were subsequently investigated via an informatic approach in order to determine the function of the gene, in addition to any genes which are common targets and/or regulators of the unique RAMs of interest in the precancerous and tumor tissue. A functional summary of these RAMs (Supplemental Fig. S5), plus four representative pathways of individual unique precancerous and tumor RAMs, are presented as Supplemental Information (Figs. S6–S9).

Many (59 of the 75 total genes and genomic regions) annotated RAMs could unambiguously be assigned a specific methylation status (Table 1). Unambiguous carry forward hypomethylations were observed in both the precancerous and tumor tissue: annexin A4 (*Anxa4*), coiled-coil domain containing 134 (*Ccdc134*), exosome component 2 (*Exosc2*), RIKEN cDNA 1700027D21 gene (*1700027D21Rik*), and c-abl oncogene 1, receptor tyrosine kinase (*Abl1*). Hypomethylated RAMs that occurred only in the tumor tissue included cellular retinoic acid binding protein 1 (*Crabp1*), nudC domain containing 3 (*Nudcd3*), protein kinase C, epsilon (*Prkce*), p53 and DNA damage regulated 1 (*Pdrg1*), solute carrier family 11 (proton-coupled divalent metal ion transporters), member 2 (*Slc11a2*), spermatogenesis associated 21 (*Spata21*), tubulin tyrosine ligase-like family, member 9, 381 bp (*Ttll9*), solute carrier family 38, member 9 (*Slc38a9*), dead box polypeptide 54 (*Ddx54*), and WSC domain containing 1, 407 bp (*Wscd1*).

RAMs that were unambiguously assigned a hypermethylated status in the precancerous tissue included dead box polypeptide 54 (*Ddx54*) and Yip1 interacting factor homolog A (*Saccharomyces cerevisiae*) (*Yif1a*). In the tumor tissue, Yip1 interacting factor homolog A (*S. cerevisiae*) (*Yif1a*) was hypermethylated. Furthermore, unambiguous new methylations in the precancerous tissue were branched chain aminotransferase 2, mitochondrial (*Bcat2*), ubiquinol-cytochrome *c* reductase (6.4 kDa) subunit (*Uqcr*), zinc finger and BTB domain containing eight opposite strand (*Zbtb8os*), chimerin (chimaerin) 2 (*Chn2*), RIKEN cDNA 1520401A03 gene (*1520401A03Rik*), sine oculis-related homeobox 3 homolog (Drosophila) (*Six3*), and WSC domain containing 1, 407 bp (*Wscd1*). Newly methylated RAMs in the tumor tissue included chimerin (chimaerin) 2 (*Chn2*), RIKEN cDNA 1520401A03 gene (*1520401A03Rik*), sine oculis-related homeobox 3 homolog (Drosophila) (*Six3*), A disintegrin-like and metallopeptidase (reprolysin type) with thrombospondin type 1 motif, 17 (*Adamts17*), annexin A2 (*Anxa2*), BTB (POZ) domain containing 11 (*Btbd11*), chemokine (C-C- motif) receptor 4 (*Ccr4*), calsyntenin 2 (*Clstn2*), folliculin (*Flcn*), glutamate decarboxylase-like 1 (*Gadl1*), Hect domain and RLD 3 (*Herc3*), like-glycosyltransferase (*Large*), leucine rich repeat and Ig domain containing 2 (*Lingo2*), src-related kinase lacking C- and N-terminal myristylation sites (*Srms*), transcription factor 4 (*Tcf4*), tubulin tyrosine ligase-like family, member 9, 208 bp (*Ttll9*), WD repeat domain 17 (*Wdr17*), zinc finger and SCAN domain containing 22 (*Zscan22*) and RIKEN cDNA A430078G23 gene (*A430078G23Rik*). There were no unambiguous hypermethylated or newly methylated RAMs that carried forward from the precancerous to the tumor tissue.

As described in the methods, some genes and genomic regions, which are greater than 10 kb away from a known gene, are tentatively classified as having multiple methylation statuses in either the precancerous or tumor tissue (21%, 16 of the 75 total genes and genomic regions). Table 1 indicates the methylation statuses and particular treatment periods at which these genes displayed altered methylation. The genes were: DNA segment, Chr 13, Wayne State University 177, expressed (*D13Wsu177e*), HIG1 domain family, member 2A (*Higd2a*), protein tyrosine phosphatase, receptor type O (*Ptpro*), dipeptidylpeptidase 10 (*Dpp10*), tyrosine kinase nonreceptor 2 (*Tnk2*), ephrin B2 (*Efnb2*), predicted gene, EG622408 (*EG622408*), prickle-like 2 (*Drosophila*) (*Prickle2*), triple functional domain, PTPRF interacting (*Trio*), transmembrane protein 132d (*Tmem132d*), and WSC domain containing 1, 359–361 bp (*Wscd1*).

There were three PCR products which each associated with multiple "hits" that displayed the highest BLAT scores (i.e., numerous genomic regions showed the fewest mismatches as compared with the sequence of interest), indicating that any of one of the various regions could correspond to the PCR product sequence. Although all of the top hits for a particular PCR product represented regions on different chromosomes, the

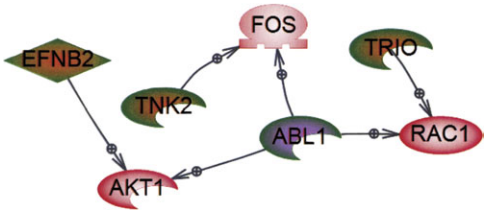

FIG. 1. Common targets of genes identified from unique regions of altered DNA methylation (RAMs) in PB-induced precancerous liver tissue from C3H/He CAR WT mice. An informatic approach was utilized to discern targets of two or more genes identified from unique PB-induced RAMs in precancerous tissue (23 weeks). Red symbols are common targets of the unique RAMs. The arrows point away from the unique RAM and towards the common target; positive arrows (—⊕→) indicate that the RAM positively affects the target. Unique RAMs are hypomethylated (green) or hypermethylated (orange). A combination of colors (i.e., green and orange) depicts a RAM with an ambiguous methylation status in the precancerous tissue. A RAM with a pink center depicts a carry forward RAM from precancerous to tumor tissue. The shapes of the entities represent the specific class of molecules to which the RAM or common target belongs: extracellular proteins or nuclear receptors (), ligands (), kinases (), and transcription factors ().

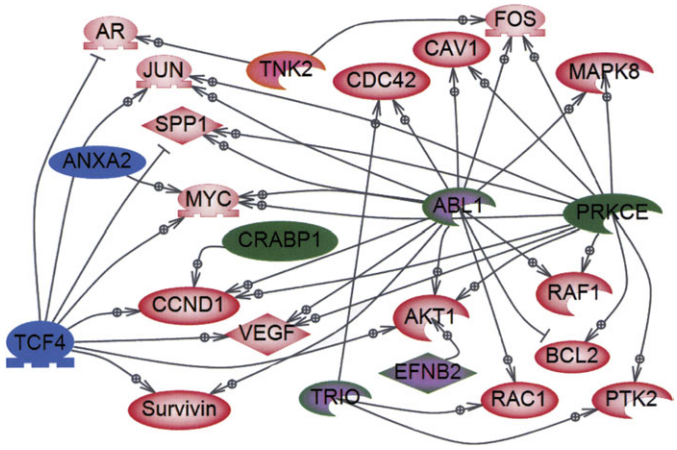

FIG. 2. Common targets of genes identified from unique regions of altered DNA methylation (RAMs) in PB-induced liver tumor tissue from C3H/He CAR WT mice. An informatic approach was utilized to discern targets of two or more genes identified from unique PB-induced RAMs in tumor tissue (32 weeks). Red symbols are common targets of the unique RAMs. The arrows point away from the unique RAM and towards the common target; positive arrows (—⊕→) indicate that the RAM positively affects the target, whereas negative arrows (—⊣) denote a negative effect. Unique RAMs are hypomethylated (green), hypermethylated (orange), or newly methylated (blue). A RAM with a pink center depicts a carry forward RAM from precancerous to tumor tissue. The shapes of the entities represent the specific class of molecules to which the RAM or common target belongs: extracellular proteins or nuclear receptors (), ligands (), kinases (), and transcription factors ().

product aligned to the identical repetitive element. Therefore, these three RAMs (442–445, 462, and 491 bp) appear to be linked to a different, specific repetitive element, and we are unable to determine with certainty which genomic region the unique RAM represents. BLAT searches revealed that regions of the genome (including the aforementioned 491 bp region), represented by 24 RAMs, are uncharacterized (i.e., located more than 10 kb away from an annotated gene). Of these 24 RAMs, the methylation statuses of 18 were unambiguous and therefore could be classified as either hypo- (five RAMs), hyper- (three RAMs), or new- (ten RAMs) methylations at a particular time point. One of the 24 uncharacterized RAMs could be assigned a specific methylation in both the precancerous and tumor tissue; the changes were opposite in direction (i.e., the precancerous RAM was hypomethylated and the tumor RAM was newly methylated). Finally, for 5 out of the 24 uncharacterized RAMs, the methylation status in the precancerous tissue (two RAMs) or the tumor tissue (three RAMs) was ambiguous.

The Pathway Studio 5.0 informatic program was used to identify common targets and regulators of these genes in precancerous and tumor tissue. Figure 1 depicts the common targets of several of the genes of interest in the precancerous tissue. Genes identified from PB-induced RAMs discerned in precancerous liver (Table 1) which do not possess targets that are in common with any of the other precancerous genes are not represented in Figure 1. Common targets of the genes identified from PB-induced RAMs discerned in tumor tissue are depicted in Figure 2. For example, Cyclin D1 (*Ccnd1*) is a common target of *Abl1*, *Crabp1*, *Prkce* and *Tcf4*, and similarly, v-akt murine thymoma viral oncogene homolog 1 (*Akt1*) is a common target of *Abl1*, *Efnb2*, *Prkce*, and *Tcf4*. In this way, potential targets of multiple genes of interest were ascertained in order to determine whether common cellular processes might be affected which could more efficiently facilitate tumorigenesis. Additionally, common regulators of genes of interest in the precancerous (Supplemental Fig. S10) and tumor (Supplemental Fig. S11) tissue were identified. In order to elucidate how these genes might be contributing to tumorigenesis, interconnections between them and five key cancer-related processes (angiogenesis, apoptosis, epithelial-mesenchymal cell transition, migration/invasion/metastasis and growth/survival) were discerned (Figs. 3–7). The genes of interest that were identified in the precancerous and tumor tissue which are linked to a particular process are depicted separately within each figure. Supplemental Information (Figs. S12-S21) contains color versions of these figures (plus the corresponding legends); the colors of the RAMs represent their methylation statuses. Additionally, the relationships depicted are referenced; numbers are noted in the figures, and the citations corresponding to the numbers are listed in Supplemental Table S2. Table 2 summarizes the potential effects of these genes on tumorigenesis, based on their connections to the aforementioned processes and their methylation statuses, assuming that methylation changes affect gene expression (e.g., increases in methylation silence expression and decreases in methylation facilitate expression).

As described in the Methods, unique B6C3F1 RAMs at 2 and 4 weeks (identified in Bachman *et al.*, 2006b; annotated in Phillips and Goodman, 2008), which corresponded to identical genes and uncharacterized genomic regions (i.e., regions of

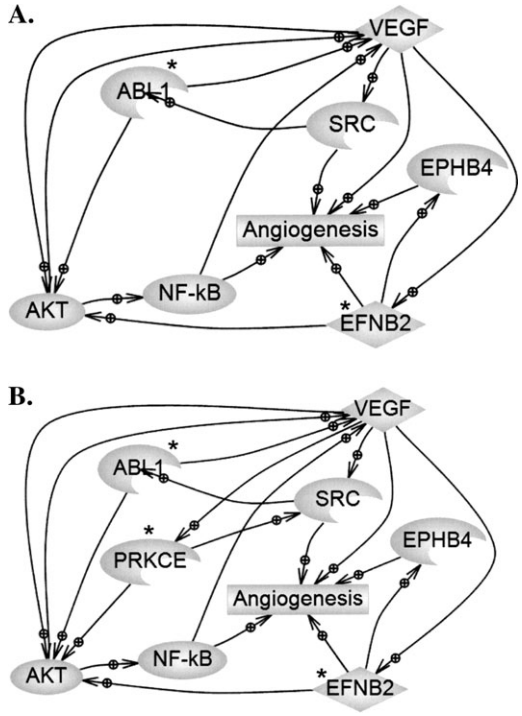

FIG. 3. Genes which exhibited altered methylation uniquely in PB-induced precancerous and liver tumor tissue and which are potentially involved in the regulation of angiogenesis. An informatic approach was utilized to discern relationships between angiogenesis and unique RAMs in precancerous (A) and tumor (B) tissue. Unique RAMs are denoted by asterisks (*). Positive arrows (⟶) indicate that an entity positively affects another gene, and/or angiogenesis directly. The shapes of the entities represent the specific class of molecules to which the RAM or connecting entity belongs: extracellular proteins or nuclear receptors (⬭), ligands (◇), and kinases (◠). Figures S12 and S13 contain color versions of (A) and (B), respectively; the colors of the RAMs represent their methylation statuses. Additionally, the relationships depicted are referenced; numbers are noted in the figures, and the citations corresponding to the numbers are listed in Supplemental Table S2.

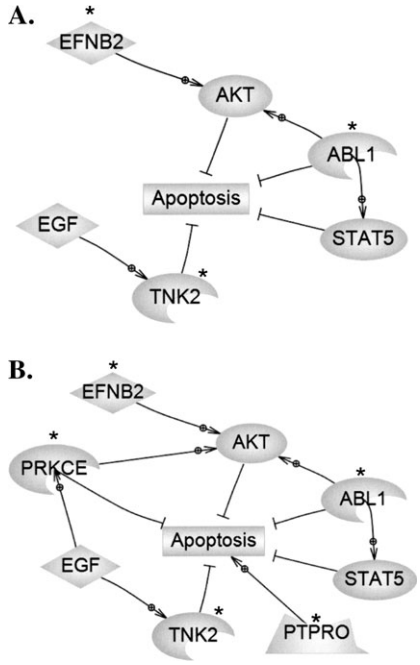

FIG. 4. Genes which exhibited altered methylation uniquely in PB-induced precancerous and liver tumor tissue and which are potentially involved in the regulation of apoptosis. An informatic approach was utilized to discern relationships between apoptosis and unique RAMs in precancerous (A) and tumor (B) tissue. Unique RAMs are denoted by asterisks (*). Positive arrows (⟶) indicate whether an entity positively affects another gene, and/or apoptosis directly, and the negative arrows (⟞) denote a negative effect. The shapes of the entities represent the specific class of molecules to which the RAM or connecting entity belongs: extracellular proteins or nuclear receptors (⬭), ligands (◇), kinases (◠), and phosphatases (⬠). Figures S14 and S15 contain color versions of (A) and (B), respectively; the colors of the RAMs represent their methylation statuses. Additionally, the relationships depicted are referenced; numbers are noted in the figures, and the citations corresponding to the numbers are listed in Supplemental Table S2.

DNA greater than 10 kb away from an annotated gene observed in the current study, were compared with the unique CAR precancerous and tumor RAMs, in order to determine whether the methylation patterns of common genes/genomic regions seen in both studies were altered similarly or differently by PB treatment. Eleven genes (*Bcat2*, *Ddx54*, *Efnb2*, *Prickle2*, *Ptpro*, *Srms*, *Tcf4*, *Tnk2*, *Trio*, *Wscd1*, and *Zscan22*), identified from unique RAMs, were observed in both groups of mice (Table 3). Five genes were identified from RAMs whose methylation statuses either clearly increase (*Bcat2*: M464-468 and *Zscan22*: H238–239) or clearly decrease (*Ddx54:*B312-315, *Ptpro*: B341–342 and *Wscd1*: M358–359) in both the B6C3F1 and CAR WT mice. Three genes were identified from RAMs whose methylation statuses are clearly opposite (e.g., increases in one group and decreases in another) in at least 1 B6C3F1 group and one CAR WT group: *Ddx54* (M315-317), *Tcf4* (H200) and *Tnk2* (M275–276). *Prickle2* (B310-312), and *Tcf4* (B200) were identified from RAMs in the B6C3F1 whose methylation statuses increase at 2 weeks, decrease at 4 weeks, and either increase (*Tcf4*) or decrease (*Prickle2*) in the CAR tumor tissue. *Wscd1* (B357–358) was identified from RAMs in the CAR precancerous and tumor tissue whose methylation statuses increase and decrease, respectively, and also increase in the B6C3F1 at 4 weeks. Finally, *Efnb2* (M564–566), *Prickle2* (H310-312), *Ptpro* (H340–343), *Srms* (M202–206), and *Trio* (M564–566) were identified from a RAM in at least one group whose methylation status is unclear after "combining" multiple RAMs (i.e., two RAMs formed in the same group and the methylation changes are opposite in direction), and thus, it is uncertain whether the altered methylation patterns in these five genes, identified from five RAMs, are similar across groups of B6C3F1 and CAR WT mice.

Six uncharacterized genomic regions on 6 different chromosomes (271–272, 288, 324, 370, 378–379, and 575–576 bp), identified from unique RAMs, were observed in both groups of mice (Supplemental Table S3). Two regions were identified from RAMs whose methylation statuses clearly decrease (271–272 bp: M270–272 and 378–379 bp: M378-380) in both

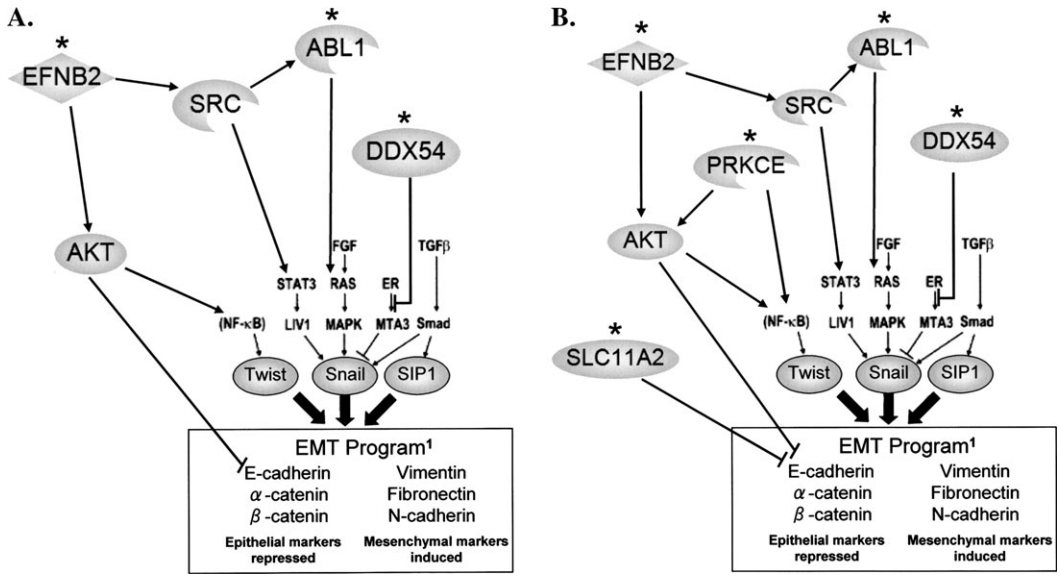

FIG. 5. Genes which exhibited altered methylation uniquely in PB-induced precancerous and liver tumor tissue and which are potentially involved in the regulation of EMT. An informatic approach was utilized to discern relationships between EMT and unique RAMs in precancerous (A) and tumor (B) tissue. Unique RAMs are denoted by asterisks (*). The positive arrows (⟶) indicate whether an entity positively affects another gene, and/or EMT directly; the negative arrows (⟞) denote a negative effect. The shapes of the entities from the modified section of the diagram represent the specific class of molecules to which the RAM or connecting entity belongs: extracellular proteins or nuclear receptors (⬭), ligands (◇), and kinases (⬭). Figures S16 and S17 contain color versions of (A) and (B), respectively; the colors of the RAMs represent their methylation statuses. Additionally, the relationships depicted are referenced; numbers are noted in the figures, and the citations corresponding to the numbers are listed in Supplemental Table S2. The annotated RAMs depicted have been superimposed on a modification of a schematic of the EMT program (Zvaifler, 2006).

the B6C3F1 and CAR WT mice. Two regions were identified from RAMs whose methylation statuses are clearly opposite (i.e., increases in one group and decreases in another) in at least one B6C3F1 group and one CAR WT group: 288 bp (M286) and 324 bp (M323–326). Regions 271–272 bp (B269-272) and 575–576 bp (M577–579) were identified from RAMs in the B6C3F1 whose methylation statuses are opposite at 2 and 4 weeks, and either increase (271–272 bp) or decrease (575–576 bp) in the CAR tumor tissue. Finally, regions 272–271 bp (H269–272) and 370 bp (B368–370) were identified from a RAM in one group whose methylation status is unclear after ''combining'' multiple RAMs (e.g., two RAMs formed in the same group and the methylation changes are opposite in direction), and thus, it is uncertain whether the altered methylation in these two cases is similar across groups of B6C3F1 and CAR WT mice.

DISCUSSION

The methodology employed in this study to evaluate PB-induced altered methylation represents an unbiased approach in the sense that the genes/genomic regions evaluated are not predetermined, that is, methylation changes are detected first, followed by the identification of the genes/genomic regions exhibiting the changes. RAMs were detected using DNA isolated from whole liver tissue for four of the experimental groups (CAR WT 23-week control, CAR KO 23-week control, CAR WT 23-week PB (precancerous) and CAR KO 23-week PB). DNA from individual liver tumors was analyzed for the fifth group, CAR WT 32-week PB. It is vital to focus upon whole animal studies, as compared with *in vitro* models only. Firstly, interactions between various cell types are likely to be essential for tumorigenesis, and whole animals also possess an intact immune system, for example, secretion of IL-6 by macrophages facilitates DEN-induced hepatocarcinogenesis (Naugler *et al*., 2007) and stromal fibroblasts can promote tumor growth (Orimo *et al*., 2005). Secondly, the origin of liver tumor cells is unclear. Cancer cell precursors are likely hepatocytes, which can proliferate in response to treatment with mitogens such as PB (Counts *et al*., 1996; Kolaja *et al*., 1996a), or partial hepatectomy (Steer, 1995), and adult human (Takahashi *et al*., 2007) and murine embryonic (Wernig *et al*., 2007) fibroblasts can be reprogrammed, producing induced pluripotent stem (iPS) cells. Importantly, iPS cells were generated from adult murine hepatocytes following transduction with only four genes, Oct 3/4, Sox2, Klf4, and c-Myc (Aoi *et al*., 2008). The reprogramming of adult pancreatic exocrine cells into induced β-cells via expression of three transcription factors: Ngn3, Pdx1, and Mafa (Zhou *et al*., 2008) provides a basis for speculating that liver cancer progenitor cells could arise directly from normal liver cells without reverting to a stem cell state. Additionally, PB treatment can inhibit hepatocyte proliferation, providing an opportunity for

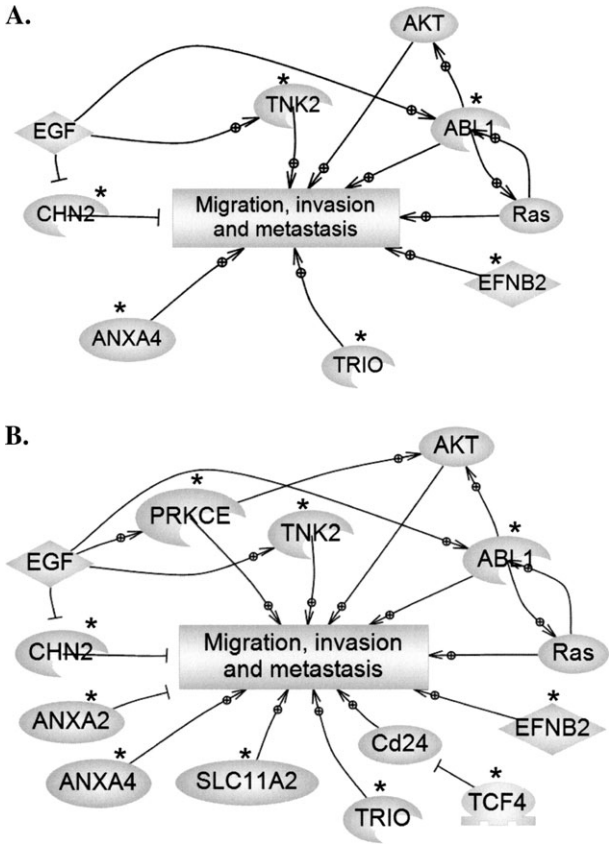

FIG. 6. Genes which exhibited altered methylation uniquely in PB-induced precancerous and liver tumor tissue and which are potentially involved in the regulation of migration, invasion and/or metastasis. An informatic approach was utilized to discern relationships between migration/invasion/metastasis and unique RAMs in precancerous (A) and tumor (B) tissue. Unique RAMs are denoted by asterisks (*). The positive arrows (⟶) indicate whether an entity positively affects another gene, and/or migration/invasion/metastasis directly, and the negative arrows (⊣) denote a negative effect. The shapes of the entities represent the specific class of molecules to which the RAM or connecting entity belongs: extracellular proteins or nuclear receptors (⬭), ligands (◇), transcription factors (⬭), and kinases (⬭). Figures S18 and S19 contain color versions of (A) and (B), respectively; the colors of the RAMs represent their methylation statuses. Additionally, the relationships depicted are referenced; numbers are noted in the figures, and the citations corresponding to the numbers are listed in Supplemental Table S2.

those cells which "lose" responsiveness to this inhibition to, possibly, form the initial clones of precancerous cells (reviewed in Counts *et al.*, 1996). The suggestion that hepatocytes are liver tumor cell precursors is not incompatible with the notion that tumor cells might originate from stem cell transformation (Reya *et al.*, 2001).

A limited number of genes have been associated with mouse liver tumorigenesis, that is, CAR (Huang *et al.*, 2005; Yamamoto *et al.*, 2004), β-catenin (Aydinlik *et al.*, 2001; Strathmann *et al.*, 2006), *c-Myc* (Vorce and Goodman, 1991), Ha-*ras* (Counts *et al.*, 1997; Vorce and Goodman, 1991; Wiseman *et al.*, 1986), Ki-*ras* (Vorce and Goodman, 1991), and *Raf* (Ray *et al.*, 1994). Previously, 146 total unique RAMs were observed in liver tumor–susceptible PB-treated CAR WT mice (precancerous and tumor tissue), as compared with their resistant KO counterpart and we suggested that, at least some of, these changes might be playing critical roles in the carcinogenesis process (Phillips *et al.*, 2007). In this study, cloning and annotation of a subset (82%) of these unique RAMs revealed 47 genes which might contribute to tumorigenesis due to their altered DNA methylation statuses; 17 have previously been implicated in cancer or related processes (Table 1). Thus, we have identified 30 "new" candidate genes which might be involved in PB-induced carcinogenesis.

We recently identified 170 unique RAMs in liver tumor-prone B6C3F1, as compared with relatively resistant C57BL/6, mice upon treatment with 0.05% PB (wt/wt) for 2 or 4 weeks (Bachman *et al.*, 2006b); subsequent cloning and annotation of these RAMs uncovered 51 genes that exhibited altered methylation (Phillips and Goodman, 2008). The combined data from these two model systems have revealed the formation of unique RAMs in liver tumor-sensitive mice at early (i.e., 2 and 4 weeks) as well as later (i.e., 23 weeks, precancerous and 32 weeks, tumor tissue) treatment time points, and thus, we have (1) evaluated methylation changes which occur within a continuum of PB-induced liver tumorigenesis, and (2) identified the genes/genomic regions that harbor these modifications.

Strikingly, there were multiple RAMs cloned in both the CAR WT and B6C3F1 mice which aligned to the exact same genomic regions and exhibited unique alterations in methylation in livers of both groups of tumor-susceptible mice, that is, B6C3F1 and CAR WT. Specifically, 11 genes were identified from identical, unique PB-induced RAMs that formed in both C3H/He CAR WT (precancerous liver and/or liver tumor) and B6C3F1 (2- and/or 4-week treated) mice (Table 3). Importantly, these similarities were observed regardless of the stock/strain of mice. Although six of these genes (*Efnb2*, *Prickle2*, *Ptpro*, *Tcf4*, *Tnk2*, and *Trio*) have previously been shown to be involved in cancer or cancer-related processes (Table 1; Supplemental Figs. S22-S27), the remaining 5 (*Bcat2*, *Ddx54*, *Srms*, *Wscd1*, and *Zscan22*) are of particular interest because they represent "new" candidate genes potentially involved in both relatively early and late stages of tumorigenesis. The androgen receptor (*AR*) and *Akt1* are common targets (Supplemental Fig. S28), whereas *Egf* is a common regulator (Supplemental Fig. S29), of a subset of the 6 cancer-related genes. For some of these common genes (*Ddx54*: M315-317, *Tcf4*: H200, and *Tnk2*: M275–76), the change in methylation status at the 2/4-week time point(s) does not occur in the same direction (e.g., hypomethylation vs. hypermethylation) as that seen in the precancerous/tumor tissue, indicating the possibility for them to have a different role during early, as compared with late, stages of tumorigenesis.

Based on these data, it is conceivable that an "altered methylation fingerprint," consisting of a subset of the genes which exhibited PB-induced altered methylation uniquely in the liver tumor-sensitive mice, could be developed and utilized

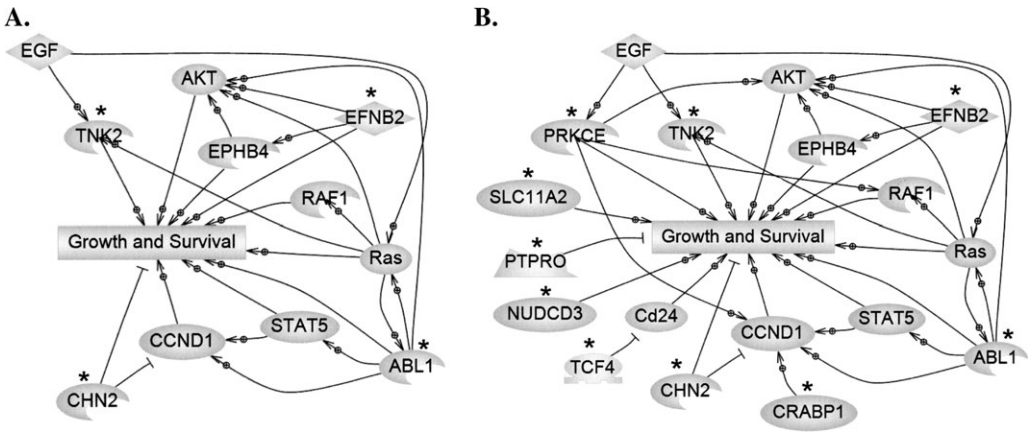

FIG. 7. Genes which exhibited altered methylation uniquely in PB-induced precancerous and liver tumor tissue and which are potentially involved in the regulation of growth/survival. An informatic approach was utilized to discern relationships between growth/survival and unique RAMs in precancerous (A) and tumor (B) tissue. Unique RAMs are denoted by asterisks (*). The positive arrows (—⊕→) indicate whether an entity positively affects another gene, and/or growth/survival directly, and the negative arrows (—⊣) denote a negative effect. The shapes of the entities represent the specific class of molecules to which the RAM or connecting entity belongs: extracellular proteins or nuclear receptors (⬭), ligands (◇), kinases (◠), phosphatases (▱), and transcription factors (⬭). Figures S20 and S21 contain color versions of (A) and (B), respectively; the colors of the RAMs represent their methylation statuses. Additionally, the relationships depicted are referenced; numbers are noted in the figures, and the citations corresponding to the numbers are listed in Supplemental Table S2.

as a biomarker to identify PB-like nongenotoxic liver tumor promoters at relatively early times following treatment. Preliminary candidates for the "altered methylation fingerprint" are those genes, presented in Table 3, which revealed identical methylation changes in both the B6C3F1 and CAR WT mice: *Bcat2*: M464-468, *Ddx54:* B312-315, *Ptpro*: B341–342, *Wscd1*: M358–359, and *Zscan22*: 238–239. Pathway diagrams of *Bcat2* and *Ptpro* are located in Supplemental Information (Figs. S30 and S24, respectively). Due to the dearth of literature information on *Wscd1* and *Zscan22*, pathways could not be generated for them. A second tier of potential genes that might contribute to an "altered methylation fingerprint" includes three genes (identified from four RAMs) which occurred in both the B6C3F1 and CAR WT mice; RAMs from at least one time point in each group exhibited similar methylation changes, however, an additional group showed an opposite or ambiguous change (e.g., from Table 3: *Prickle2*: H310-312, excluding the ambiguous precancerous RAM, *Prickle2*: B310-312, excluding the B6C3F1, 2-week RAM, *Tcf4*: B200, excluding the B6C3F1, 4-week RAM, and *Wscd1*: B357–358, excluding the tumor RAM). Pathway diagrams of *Prickle2* and *Tcf4* are located in Supplemental Information (Figs. S23 and S25, respectively).

Although the genes exhibiting unique PB-induced altered methylation patterns in the precancerous and tumor tissue may individually be playing crucial roles during tumorigenesis (e.g., hypermethylation of a growth suppressor or hypomethylation of an oncogene), analysis of total hepatic DNA, or DNA isolated from individual tumors, does not allow us to conclude whether the changes occurred in one, or multiple, cell populations. Because it is possible that these modifications arose in different populations, it is constructive to consider the overarching pathways (e.g., angiogenesis) in which these genes participate (Table 2; Figs. 3–7; Supplemental Figs. S12–S21). Similar observations were made by Jones *et al*. (2008) and Parsons *et al*. (2008), who showed that core signaling pathways were genetically altered in pancreatic cancer and glioblastoma, respectively. Importantly, although the particular mutations varied among tumor samples of a specific cancer type (i.e., different genes were affected, depending on the sample), the altered genes participate in the same pathways. Likewise, epigenetic deregulation of certain pathways by numerous genes identified from unique RAMs might more efficiently facilitate tumor formation. Importantly, several unique precancerous RAMs are involved in five distinct processes, however, more unique RAMs in the tumor tissue potentially affect these same pathways (Figs. 3–7), suggesting that altered methylation plays progressively critical roles during tumor development. Additionally, common targets of multiple unique RAMs in the precancerous (Fig. 1) and tumor (Fig. 2) tissue suggest that common processes might be influenced, for example, AKT1 is a common target of 4 genes identified from unique RAMs in the tumor tissue (Fig. 2: *Abl1*, *Efnb2*, *Prkce*, and *Tcf4*).

Of the five the processes in which multiple genes identified from unique precancerous and tumor RAMs are involved (Figs. 3–7), four of them (angiogenesis, EMT, growth/survival, and invasion/metastasis) are also converged upon by unique B6C3F1 RAMs at 2 or 4 weeks of PB treatment (Fig. 4 in Phillips and Goodman, 2008). Furthermore, common targets (AKT1, CCND1, FOS, JUN, PTK2, and VEGF) of unique precancerous and/or tumor RAMs (Figs. 1 and 2) are also targets of unique B6C3F1, 4-week RAMs (Fig. 3 in Phillips and Goodman, 2008). These data, combined with the finding that several common genes in the B6C3F1 (2 and 4 weeks) and

TABLE 2
Genes Identified from Unique PB-induced RAMs in C3H/He CAR WT (Precancerous Liver and/or Liver Tumor), as compared with Resistant CAR KO Mice, and their Potential Functional Significance in Tumorigenesis

Cell process or gene[a]	Methylation status in precancerous[b]	Methylation status in tumor[c]	Potential effect of the RAM on indicated process[d]	
			Precancerous	Tumor
Angiogenesis				
Abl1[e]	Carry forward HypoM	Carry forward HypoM	↑[f]	↑
Efnb2	Carry forward HypoM and/or HyperM	Carry forward HypoM and/or HypoM	↑ or ↓[g]	↑
Prkce		HypoM		↑
Apoptosis				
Abl1	Carry forward HypoM	Carry Forward HypoM	↓	↓
Efnb2	Carry forward HypoM and/or HyperM	Carry forward HypoM and/or HypoM	↓ or ↑	↓
Tnk2	HypoM and/or carry forward HyperM	Carry forward HyperM	↓ or ↑	↑
Prkce		HypoM		↓
Ptpro		HypoM and/or NewM		↑ or ↓
Epithelial-mesenchymal transition				
Abl1	Carry forward HypoM	Carry Forward HypoM	↑	↑
Ddx54	HyperM	HypoM	↓	↑
Efnb2	Carry forward HypoM and/or HyperM	Carry forward HypoM and/or HypoM	↑ or ↓	↑
Prkce		HypoM		↑
Slc11a2		HypoM		↑
Growth/survival				
Abl1	Carry forward HypoM	Carry Forward HypoM	↑	↑
Chn2	NewM	NewM	↑	↑
Efnb2	Carry forward HypoM and/or HyperM	Carry forward HypoM and/or HypoM	↑ or ↓	↑
Tnk2	HypoM and/or carry forward HyperM	Carry forward HyperM	↑ or ↓	↓
Crabp1		HypoM		↑
Nudcd3		HypoM		↑
Prkce		HypoM		↑
Ptpro		HypoM and/or NewM		↓ or ↑
Slc11a2		HypoM		↑
Tcf4		NewM		↑
Migration/invasion/metastasis				
Abl1	Carry forward HypoM	Carry forward HypoM	↑	↑
Anxa4	Carry forward HypoM	Carry forward HypoM	↑	↑
Chn2	NewM	NewM	↑	↑
Efnb2	Carry forward HypoM and/or HyperM	Carry forward HypoM and/or HypoM	↑ or ↓	↑
Tnk2	HypoM and/or carry forward HyperM	Carry forward HyperM	↑ or ↓	↓
Trio	HyperM and/or carry forward HypoM	HypoM and/or carry forward HypoM	↓ or ↑	↑
Anxa2		NewM		↑
Prkce		HypoM		↑
Slc11a2		HypoM		↑
Tcf4		NewM		↑

[a]Genes which were identified from one or more unique RAMs discerned in precancerous and tumor tissue.
[b]Methylation statuses of genes in precancerous tissue (23 weeks of PB treatment).
[c]Methylation statuses of genes in tumor tissue (32 weeks of PB treatment).
[d]Based on methylation status(es) of the genes (assuming that increases in methylation silence expression and decreases in methylation facilitate expression), and the relationships between the genes and a cellular process (Figs. 3–7, and Supplemental Figs. S12-S21).
[e]Specific relationships between a gene and cellular process are depicted in Figures 3–7 and Supplemental Figures S12-S21, and the corresponding references are listed in Supplemental Table S2.
[f]A ↑ symbol indicates a potential positive effect (including positive regulation, and inhibition of negative regulation) of the RAM on a cellular process.
[g]A ↓ symbol indicates a potential negative effect (including negative regulation, and inhibition of positive regulation) of the RAM on a cellular process.

CAR WT (23 and 32 weeks) mice exhibited PB-induced altered methylation (Table 3), indicate the importance of early modifications which might ultimately influence expression and drive tumorigenesis.

Many genes exhibit point mutations, deletions or amplifications in various cancers (Jones *et al.*, 2008; Parsons *et al.*, 2008). However, the integration of genetic and epigenetic data are crucial to understanding the molecular basis of the disease

TABLE 3
Genes Identified from Identical, Unique PB-induced RAMs that Formed in both CAR WT (Precancerous Liver and/or Liver Tumor) and B6C3F1 (2- and/or 4-Week Treated) Mice.

		Methylation status			
		B6C3F1[a]		CAR WT[b]	
Gene (genomic classification)	Considered to be one RAM	2 weeks	4 weeks	Precancerous	Tumor
Bcat2: Branched chain aminotransferase 2, mitochondrial (1.A.ii: Exonic)	M464-468[c]		$\uparrow^{N}$ (M464)[d]	$\uparrow^{N}$ (M468)	
Ddx54: Dead box polypeptide 54 (1.A.iii: Intronic)	M315-317[g] B312-315[g]		↓ (M317)[e]	↑ (M315)	↓ (B312)
Efnb2: Ephrin B2 (1.A.iii: Intronic)	M564-566	↓ (M566) or $\uparrow^{N}$ (M565)[f]	↓ (B315)	↑ (M564)	↓ (M564)
Prickle2: Prickle-like 2 (*Drosophila*) (1.B.ii: >2 and ≤10 kb upstream from TSS)	H310-312[g] B310-312[g]	↓ (H312) $\uparrow^{N}$ (B310)	↓ (H310) ↓ (B310)	↓ (H310) or ↑ (H312)[f]	↓ (H312) ↓ (B312)
Ptpro: Protein tyrosine phosphatase, receptor type O (1.A.iii: Intronic)	H340-343[g] B341-342[g]	↓ (H341) or $\uparrow^{N}$ (H343)[f] ↓ (B341)	↓ (B341)		↓ (H342) or $\uparrow^{N}$ (H340)[f] ↓ (B342)
Srms: src-related kinase lacking C-terminal regulatory tyrosine and N-terminal myristylation sites (1.A.i: Spans TSS and/or 5′ UTR)	M202-206	↑ (M202) or ↓ (M206)[f]			$\uparrow^{N}$ (M205)
Tcf4: Transcription factor 4 (1.A.iii: Intronic)	H200[g] B200[g]	↓ (H200) ↑ (B200)	 ↓ (B200)		$\uparrow^{N}$ (H200) $\uparrow^{N}$ (B200)
Tnk2: Tyrosine kinase nonreceptor 2 (1.A.iii: Intronic)	M275–276		↓ (M275)	↑ (M276)	↑ (M276)
Trio: Triple functional domain (PTPRF interacting) (1.A.ii: Exonic)	M564-566	↓ (M566) or $\uparrow^{N}$ (M565)[f]		↑ (M564)	↓ (M564)
Wscd1: WSC domain containing 1 (359–361 bp) (1.A.iii: Intronic)	M358–359[g] B357–358[g]		↓ (M358) ↑ (B357)	 $\uparrow^{N}$ (B357)	↓ (M359) ↓ (B358)
Zscan22: Zinc finger and SCAN domain containing 22 (1.A.i.: Spans TSS and/or 5′ UTR)	H238–239		$\uparrow^{N}$ (H238 or H239)[h]		$\uparrow^{N}$ (H238)

[a]Unique RAMs that formed in livers of B6C3F1 mice upon 2 or 4 weeks of 0.05% (wt/wt) PB treatment.

[b]Unique RAMs that formed in C3H/He CAR WT (precancerous or tumor) liver tissue.

[c]A unique RAM (e.g., H200) is listed as a single letter, which indicates the methylation-sensitive restriction enzyme (*Bss*HII, *Hpa*II, or *Msp*I) which led to the identification of the RAM, plus the size(s), in base pairs, of the unique RAMs detected. If more than 1 size is listed, (e.g., M564–566), these represent the span of the RAM sizes in the B6C3F1 and CAR WT groups, as noted in parentheses in the ''methylation status'' column. The rationale for considering multiple RAMs of similar sizes to be one RAM is detailed within the ''Materials/Methods.'' [d]The presence of an arrow, plus the RAM size, indicates that the unique RAM was discerned in a specific group of mice. Increases in methylation (hypermethylated RAMs: those which are significant, Student's *t*-test, $p < 0.05$, and newly methylated RAMs, where PCR product formed in the treatment but not the control group) are collectively represented by an upwards arrow (↑); A^{N} depicts a new methylation, whereas hypermethylations remain as unlabeled upwards arrows.

[e]Decreases in methylation (hypomethylated RAMs, both 100% decreases, and those which are significant, Student's *t*-test, $p < 0.05$) are collectively represented by a downwards arrow (↓).

[f]The methylation status is ambiguous (e.g., newly methylated M565 or hypomethylated M566 might represent *Efnb2*).

[g]Because three different restriction digestions were utilized, more than 1 RAM might represent a single gene.

[h]The gene might be represented by 1 of 2 RAMs which exhibited the same directiion of change (e.g., both are new methylations).

(McLendon et al., 2008), and our data highlight the significance of DNA methylation as an epigenetic mechanism underlying tumorigenesis. It is known that C3H/He and B6C3F1 mice are more susceptible to liver tumors as compared with the C57BL/6 strain (Becker, 1982). In response to PB treatment, methylation patterns are altered to a greater extent in the sensitive groups, including higher levels of hypermethylation (C3H/He >> B6C3F1 > C57BL/6), and thus, it is hypothesized that the inability of these animals to maintain normal methylation patterns is responsible, at least in part, for their differential liver tumor susceptibilities (Watson and Goodman, 2002). Although the fundamental genes underlying

liver cancer in mice and humans are likely the same, rodents exhibit an increased susceptibility to tumorigenesis (Rangarajan and Weinberg, 2003). Also, it has been observed that methylation patterns in rodent cells are less stable than in human cells (reviewed in Goodman and Watson, 2002). Therefore, a difference between humans and rodents might exist with regard to the regulation of epigenetic control, including DNA methylation, resulting in enhanced sensitivity to tumor formation in the latter.

PB causes hepatic hypertrophy and hyperplasia (Whysner *et al*., 1996), and PB-treated CAR WT, but not CAR KO, mice exhibit an increase in liver mass due to mitogenesis and cellular hypertrophy (Wei *et al*., 2000). Thus, hypomethylation could result from replication-dependent, passive demethylation (Howlett and Reik, 1991). Hypomethylated RAMs might occur via physical blocking of *cis*-elements and/or *trans*-acting factors (e.g., DNA methyltransferases, DNMTs, or methyl-binding proteins) by CAR itself, for example, the presence of CAR on DNA could sterically hinder the binding of DNMT1. Active demethylation (reviewed in Ooi and Bestor, 2008) might also decrease 5-methylcytosine levels. Increases in methylation (i.e., hyper- and new methylations) could be mediated by the recruitment of de novo DNMTs (i.e., 3A and 3B) and/or methyl-binding proteins to DNA by CAR, similar to the orphan nuclear receptor GCNF recruitment of *de novo* methyltransferases, resulting in *Oct-3/4* silencing (Sato *et al*., 2006). Moreover, CAR might mediate PB-induced expression changes in proteins that could alter methylation status: DNMTs (Goll and Bestor, 2005), proteins involved in demethylation (Ooi and Bestor, 2008), methyl-binding proteins (Lopez-Serra and Esteller, 2008) and/or enzymes involved in regulating levels of *S*-adenosylmethionine (SAM), the primary methyl-donor for DNMT reactions (Ulrey *et al*., 2005).

The current study focused upon PB-induced RAMs that formed uniquely in liver tumor-sensitive CAR WT (pre-cancerous liver and/or liver tumor tissue), as compared with resistant CAR KO, mice, and the genes identified from these RAMs can function in processes that are important for tumor development, including angiogenesis, apoptosis, EMT, growth/survival, and migration/invasion/metastasis. These data, plus the results from an analogous study which discerned PB-elicited unique RAMs at 2 and 4 weeks in susceptible B6C3F1, as compared with relatively resistant C57BL/6, mice (Bachman *et al*., 2006b; Phillips and Goodman, 2008), allowed us to identify genes whose methylation statuses were altered uniquely in sensitive animals within a continuum of PB-induced liver tumorigenesis. A subset of these, as discussed above, represent our initial, preliminary candidate "altered methylation fingerprint" which might be employed as a biomarker to identify PB-like nongenotoxic liver tumor promoters at relatively early times following treatment. Common genes observed at both early (B6C3F1) and later (CAR WT) time points of treatment (Table 3), which exhibited unique PB-induced alterations in methylation, participate in the same key processes, indicating that methylation changes at early times are critical for tumor formation. Thus, the current study represents an important step forward towards our goal of enhancing our understanding of genes and pathways involved in PB-induced tumorigenesis. Expression analysis (both quantitative real-time PCR and microarrays) is currently being performed on RNA isolated from the same liver tissue used in the current study and our study involving a comparison of the effects of PB (following 2 or 4 weeks of treatment) on liver tumor–susceptible B6C3F1 mice as compared with the relatively resistant C57BL/6 (Phillips and Goodman, 2008).

SUPPLEMENTARY DATA

Supplementary data are available online at http://toxsci.oxfordjournals.org/.

FUNDING

National Institutes of Health/National Institute of Environmental Health Sciences training grant No. (T32-ES-7255) predoctoral fellowship to J.M.P.

ACKNOWLEDGMENTS

C3H/He CAR WT and KO mouse liver tissue was graciously provided by Drs Masahiko Negishi and Robert Maronpot (National Institute of Environmental Health Sciences). Research support, in the form of a gift, from the R.J. Reynolds Tobacco Company is acknowledged gratefully.

REFERENCES

Aoi, T., Yae, K., Nakagawa, M., Ichisaka, T., Okita, K., Takahashi, K., Chiba, T., and Yamanaka, S. (2008). Generation of pluripotent stem cells from adult mouse liver and stomach cells. *Science* **321,** 699–702.

Aydinlik, H., Nguyen, T. D., Moennikes, O., Buchmann, A., and Schwarz, M. (2001). Selective pressure during tumor promotion by phenobarbital leads to clonal outgrowth of beta-catenin-mutated mouse liver tumors. *Oncogene* **22,** 7812–7816.

Bachman, A. N., Kamendulis, L. M., and Goodman, J. I. (2006a). Diethanolamine and phenobarbital produce an altered pattern of methylation in GC-rich regions of DNA in B6C3F1 mouse hepatocytes similar to that resulting from choline deficiency. *Toxicol. Sci.* **90,** 317–325.

Bachman, A. N., Phillips, J. M., and Goodman, J. I. (2006b). Phenobarbital Induces progressive patterns of GC-rich and gene-specific altered DNA methylation in the liver of tumor-prone B6C3F1 mice. *Toxicol. Sci.* **91,** 393–405.

Becker, F. F. (1982). Morphological classification of mouse liver tumors based on biological characteristics. *Cancer Res.* **42,** 3918–3923.

Buchmann, A., Bauer-Hofmann, R., Mahr, J., Drinkwater, N. R., Luz, A., and Schwarz, M. (1991). Mutational activation of the c-Ha-ras gene in liver tumors of different rodent strains: Correlation with susceptibility to hepatocarcinogenesis. *Proc. Natl. Acad. Sci. U. S. A.* **88,** 911–915.

Counts, J. L., McClain, R. M., and Goodman, J. I. (1997). Comparison of effect of tumor promoter treatments on DNA methylation status and gene expression in B6C3F1 and C57BL/6 mouse liver and in B6C3F1 mouse liver tumors. *Mol. Carcinog.* **18,** 97–106.

Counts, J. L., Sarmiento, J. I., Harbison, M. L., Downing, J. C., McClain, R. M., and Goodman, J. I. (1996). Cell proliferation and global methylation status changes in mouse liver after phenobarbital and/or choline-devoid, methionine-deficient diet administration. *Carcinogenesis* **17,** 1251–1257.

Esteller, M. (2008). Epigenetics in cancer. *N. Engl. J. Med.* **358,** 1148–1159.

Fox, T. R., Schumann, A. M., Watanabe, P. G., Yano, B. L., Maher, V. M., and McCormick, J. J. (1990). Mutational analysis of the H-ras oncogene in spontaneous C57BL/6 x C3H/He mouse liver tumors and tumors induced with genotoxic and nongenotoxic hepatocarcinogens. *Cancer Res.* **50,** 4014–4019.

Goll, M. G., and Bestor, T. H. (2005). Eukaryotic cytosine methyltransferases. *Annu. Rev. Biochem.* **74,** 481–514.

Goodman, J. I., and Watson, R. E. (2002). Altered DNA methylation: A secondary mechanism involved in carcinogenesis. *Annu. Rev. Pharmacol. Toxicol.* **42,** 501–525.

Honkakoski, P., Zelko, I., Sueyoshi, T., and Negishi, M. (1998). The nuclear orphan receptor CAR-retinoid X receptor heterodimer activates the phenobarbital-responsive enhancer module of the CYP2B gene. *Mol. Cell. Biol.* **18,** 5652–5658.

Howlett, S. K., and Reik, W. (1991). Methylation levels of maternal and paternal genomes during preimplantation development. *Development* **113,** 119–127.

Huang, W., Zhang, J., Chua, S. S., Qatanani, M., Han, Y., Granata, R., and Moore, D. D. (2003). Induction of bilirubin clearance by the constitutive androstane receptor (CAR). *Proc. Natl. Acad. Sci. U. S. A.* **100,** 4156–4161.

Huang, W., Zhang, J., Washington, M., Liu, J., Parant, J. M., Lozano, G., and Moore, D. D. (2005). Xenobiotic stress induces hepatomegaly and liver tumors via the nuclear receptor constitutive androstane receptor. *Mol. Endocrinol.* **19,** 1646–1653.

Jones, S., Zhang, X., Parsons, D. W., Lin, J. C., Leary, R. J., Angenendt, P., Mankoo, P., Carter, H., Kamiyama, H., Jimeno, A., *et al.* (2008). Core signaling pathways in human pancreatic cancers revealed by global genomic analyses. *Science* **321,** 1801–1806.

Kawamoto, T., Sueyoshi, T., Zelko, I., Moore, R., Washburn, K., and Negishi, M. (1999). Phenobarbital-responsive nuclear translocation of the receptor CAR in induction of the CYP2B gene. *Mol. Cell. Biol.* **19,** 6318–6322.

Kolaja, K. L., Stevenson, D. E., Johnson, J. T., Walborg, E. F., Jr, and Klaunig, J. E. (1996a). Subchronic effects of dieldrin and phenobarbital on hepatic DNA synthesis in mice and rats. *Fundam. Appl. Toxicol.* **29,** 219–228.

Kolaja, K. L., Stevenson, D. E., Walborg, E. F., Jr, and Klaunig, J. E. (1996b). Dose dependence of phenobarbital promotion of preneoplastic hepatic lesions in F344 rats and B6C3F1 mice: Effects on DNA synthesis and apoptosis. *Carcinogenesis* **17,** 947–954.

Konno, Y., Negishi, M., and Kodama, S. (2008). The roles of nuclear receptors CAR and PXR in hepatic energy metabolism. *Drug Metab. Pharmacokinet.* **23,** 8–13.

Lopez-Serra, L., and Esteller, M. (2008). Proteins that bind methylated DNA and human cancer: Reading the wrong words. *Br. J. Cancer* **98,** 1881–1885.

McLendon, R., Friedman, A., Bigner, D., VanMeir, E. G., Brat, D. J., Mastrogianakis, G. M., Olson, J. J., Mikkelsen, T., Lehman, N., Aldape, K., *et al.* (2008). Comprehensive genomic characterization defines human glioblastoma genes and core pathways. *Nature* **455,** 1061–1068.

Moennikes, O., Buchmann, A., Romualdi, A., Ott, T., Werringloer, J., Willecke, K., and Schwarz, M. (2000). Lack of phenobarbital-mediated promotion of hepatocarcinogenesis in connexin 32-null mice. *Cancer Res.* **15,** 5087–5091.

Naugler, W. E., Sakurai, T., Kim, S., Maeda, S., Kim, K., Elsharkawy, A. M., and Karin, M. (2007). Gender disparity in liver cancer due to sex differences in MyD88-dependent IL-6 production. *Science* **317,** 121–124.

Ooi, S. K., and Bestor, T. H. (2008). The colorful history of active DNA demethylation. *Cell* **133,** 1145–1148.

Orimo, A., Gupta, P. B., Sgroi, D. C., Arenzana-Seisdedos, F., Delaunay, T., Naeem, R., Carey, V. J., Richardson, A. L., and Weinberg, R. A. (2005). Stromal fibroblasts present in invasive human breast carcinomas promote tumor growth and angiogenesis through elevated SDF-1/CXCL12 secretion. *Cell* **121,** 335–348.

Parsons, D. W., Jones, S., Zhang, X., Lin, J. C., Leary, R. J., Angenendt, P., Mankoo, P., Carter, H., Siu, I. M., Gallia, G. L., *et al.* (2008). An integrated genomic analysis of human glioblastoma multiforme. *Science* **321,** 1807–1812.

Phillips, J. M., and Goodman, J. I. (2008). Identification of genes that may play critical roles in phenobarbital (PB)-induced liver tumorigenesis due to altered DNA methylation. *Toxicol. Sci.* **104,** 86–99.

Phillips, J. M., Yamamoto, Y., Negishi, M., Maronpot, R. R., and Goodman, J. I. (2007). Orphan nuclear receptor constitutive active/androstane receptor-mediated alterations in DNA methylation during phenobarbital promotion of liver tumorigenesis. *Toxicol. Sci.* **96,** 72–82.

Rangarajan, A., and Weinberg, R. A. (2003). Comparative biology of mouse versus human cells: Modeling human cancer in mice. *Nat. Rev. Cancer* **3,** 952–959.

Ray, J. S., Harbison, M. L., McClain, R. M., and Goodman, J. I. (1994). Alterations in the methylation status and expression of the raf oncogene in phenobarbital-induced and spontaneous B6C3F1 mouse live tumors. *Mol. Carcinog.* **9,** 155–166.

Reya, T., Morrison, S. J., Clarke, M. F., and Weissman, I. L. (2001). Stem cells, cancer, and cancer stem cells. *Nature* **414,** 105–111.

Rumsby, P. C., Barrass, N. C., Phillimore, H. E., and Evans, J. G. (1991). Analysis of the Ha-ras oncogene in C3H/He mouse liver tumours derived spontaneously or induced with diethylnitrosamine or phenobarbitone. *Carcinogenesis* **12,** 2331–2336.

Sato, N., Kondo, M., and Arai, K. (2006). The orphan nuclear receptor GCNF recruits DNA methyltransferase for Oct-3/4 silencing. *Biochem. Biophys. Res. Commun.* **344,** 845–851.

Steer, C. J. (1995). Liver regeneration. *FASEB J.* **9,** 1396–1400.

Strathmann, J., Schwarz, M., Tharappel, J. C., Glauert, H. P., Spear, B. T., Robertson, L. W., Appel, K. E., and Buchmann, A. (2006). PCB 153, a non-dioxin-like tumor promoter, selects for beta-catenin (Catnb)-mutated mouse liver tumors. *Toxicol. Sci.* **93,** 34–40.

Sueyoshi, T., Kawamoto, T., Zelko, I., Honkakoski, P., and Negishi, M. (1999). The repressed nuclear receptor CAR responds to phenobarbital in activating the human CYP2B6 gene. *J. Biol. Chem.* **274,** 6043–6046.

Sueyoshi, T., Moore, R., Sugatani, J., Matsumura, Y., and Negishi, M. (2008). PPP1R16A, the membrane subunit of protein phosphatase 1beta, signals nuclear translocation of the nuclear receptor constitutive active/androstane receptor. *Mol. Pharmacol.* **73,** 1113–1121.

Sugatani, J., Kojima, H., Ueda, A., Kakizaki, S., Yoshinari, K., Gong, Q. H., Owens, I. S., Negishi, M., and Sueyoshi, T. (2001). The phenobarbital response enhancer module in the human bilirubin UDP-glucuronosyltransferase UGT1A1 gene and regulation by the nuclear receptor CAR. *Hepatology* **33,** 1232–1238.

Swales, K., and Negishi, M. (2004). CAR, driving into the future. *Mol. Endocrinol.* **18,** 1589–1598.

Takahashi, K., Tanabe, K., Ohnuki, M., Narita, M., Ichisaka, T., Tomoda, K., and Yamanaka, S. (2007). Induction of pluripotent stem cells from adult human fibroblasts by defined factors. *Cell* **131,** 861–872.

Ueda, A., Hamadeh, H. K., Webb, H. K., Yamamoto, Y., Sueyoshi, T., Afshari, C. A., Lehmann, J. M., and Negishi, M. (2002). Diverse roles of the nuclear orphan receptor CAR in regulating hepatic genes in response to phenobarbital. *Mol. Pharmacol.* **61,** 1–6.

Ulrey, C. L., Liu, L., Andrews, L. G., and Tollefsbol, T. O. (2005). The impact of metabolism on DNA methylation. *Hum. Mol. Genet.* 14 Spec No 1: R139–R147.

Vorce, R. L., and Goodman, J. I. (1991). Hypomethylation of ras oncogenes in chemically induced and spontaneous B6C3F1 mouse liver tumors. *Toxicol. Environ. Health* **34,** 367–384.

Watson, R. E., and Goodman, J. I. (2002). Effects of phenobarbital on DNA methylation in GC-rich regions of hepatic DNA from mice that exhibit different levels of susceptibility to liver tumorigenesis. *Toxicol. Sci.* **68,** 51–58.

Wei, P., Zhang, J., Egan-Hafley, M., Liang, S., and Moore, D. D. (2000). The nuclear receptor CAR mediates specific xenobiotic induction of drug metabolism. *Nature* **407,** 920–923.

Wernig, M., Meissner, A., Foreman, R., Brambrink, T., Ku, M., Hochedlinger, K., Bernstein, B. E., and Jaenisch, R. (2007). In vitro reprogramming of fibroblasts into a pluripotent ES-cell-like state. *Nature* **448,** 318–324.

Whysner, J., Ross, P. M., and Williams, G. M. (1996). Phenobarbital mechanistic data and risk assessment: Enzyme induction, enhanced cell proliferation, and tumor promotion. *Pharmacol. Ther.* **71,** 53–91.

Wiseman, R. W., Stowers, S. J., Miller, E. C., Anderson, M. W., and Miller, J. A. (1986). Activating mutations of the c-Ha-ras protooncogene in chemically induced hepatomas of the male B6C3 F1 mouse. *Proc. Natl. Acad. Sci. U. S. A.* **83,** 5825–5829.

Yamamoto, Y., Kawamoto, T., and Negishi, M. (2003). The role of the nuclear receptor CAR as a coordinate regulator of hepatic gene expression in defense against chemical toxicity. *Arch. Biochem. Biophys.* **409,** 207–211.

Yamamoto, Y., Moore, R., Goldsworthy, T. L., Negishi, M., and Maronpot, R. R. (2004). The orphan nuclear receptor constitutive active/androstane receptor is essential for liver tumor promotion by phenobarbital in mice. *Cancer Res.* **64,** 7197–7200.

Zhou, Q., Brown, J., Kanarek, A., Rajagopal, J., and Melton, D. A. (2008). *In vivo* reprogramming of adult pancreatic exocrine cells to β-cells. *Nature* **455,** 627–632.

Zvaifler, N. J. (2006). Relevance of the stroma and epithelial-mesenchymal transition (EMT) for the rheumatic diseases. *Arthritis Res. Ther.* **8,** 210–220.